

## Supporting Information

### Selective Cyclohexene Oxidation to Allylic Compounds over Cu-triazole Framework via Homolytic Activation of Hydrogen Peroxide

Panyapat Ponchai,<sup>a</sup> Kanyaporn Adpakpang,<sup>a\*</sup> and Sareeya Bureekaew<sup>a,b</sup>

<sup>a</sup> School of Energy Science and Engineering, Vidyasirimedhi Institute of Science and Technology, 555 Moo 1 Payupnai, Wangchan, Rayong 21210, Thailand.

<sup>b</sup> Research Network of NANOTEC-VISTEC on Nanotechnology for Energy, Vidyasirimedhi Institute of Science and Technology, Wangchan, Rayong, 21210, Thailand.

## Chemicals

Copper chloride dihydrate ( $\text{CuCl}_2 \cdot 2\text{H}_2\text{O}$  (Merck), 1,2,4-triazole (TCl, > 99%), acetonitrile (MeCN, Honeywell), hydrogen peroxide ( $\text{H}_2\text{O}_2$ , 30 %wt. in water), cyclohexene (CyH, Sigma-Aldrich, > 99.0%), cyclohexene oxide (**1**, Aldrich, > 98%), *trans*-1,2-cyclohexanediol (**2**, Merck), 2-cyclohexen-1-ol (**3**, Aldrich, > 95%), and 2-cyclohexen-1-one (**4**, Aldrich, > 95%) were used without further purification.

## Preparation of Cu-trz catalyst

$[\text{Cu}_3(\text{trz})_3(\mu_3\text{-OH})](\text{OH})_2 \cdot 6\text{H}_2\text{O}$  was synthesized by a microwave-assisted hydrothermal method according to the previously reported protocol with some modifications.<sup>1</sup> In a typical synthesis,  $\text{CuCl}_2 \cdot 2\text{H}_2\text{O}$  (0.68 g, 4 mmol) and 1,2,4-triazole (0.28 g, 4 mmol) were dissolved in 10 mL deionized water at room temperature under stirring. The resulting mixture was heated by microwave radiation (CEM discovery) at 100 °C for 20 min. After cooling down to room temperature, the product solution was filtered by centrifugation and washed with DI several times. The blue powder of Cu-trz was collected after drying in vacuum oven at room temperature for 12 h.

## Oxidation of cyclohexene

The liquid-phase catalytic oxidation of CyH was carried out in 10 mL capped glass-vial. In a typical reaction, CyH (200  $\mu\text{L}$ , 20 mmol) and catalyst (25mg) were added in 2 mL MeCN. The reaction was initiated by adding 250  $\mu\text{L}$  of 30 %wt.  $\text{H}_2\text{O}_2$  solution. The batch reactions were performed in an automated pressure under a constant agitation of 200 rpm. The reactions were conducted at various temperatures and reaction times to find out the optimal condition. After the reaction, the glass-vial was cooled down to room temperature in an ice-water bath. The liquid phase was filtered and diluted in MeCN prior to analyzing by gas chromatography-mass spectrometry (GC-MS). The catalytic performances were evaluated in terms of CyH conversion, product yield, and selectivity calculated based on a molar basis as follows:

$$\% \text{Conversion} = \frac{[\text{CyH}]_{\text{initial}} - [\text{CyH}]_{\text{final}}}{[\text{CyH}]_{\text{initial}}} * 100$$

$$\% \text{Yield} = \frac{[\text{Mole of product}]}{[\text{Mole of CyH}_{\text{initial}}]} * 100$$

$$\% \text{Allylic selectivity} = \frac{\text{Yield of allylic products}}{\text{Sum of products}} * 100$$

where, Yield of allylic products = Yields of **3** + **4**

Sum of products = Yields of **1** + **2** + **3** + **4**

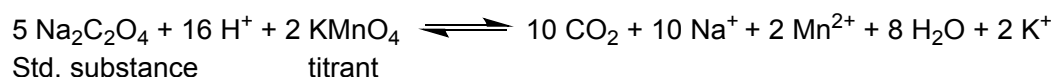
Quantitative analysis of each component was accomplished using calibration curves of commercially available chemicals.

### Characterizations

- Powder X-ray diffraction (PXRD) patterns were recorded on Bruker, New D8 Advance. Measurements were made over the range  $5^\circ < 2\theta < 40^\circ$  at room temperature using Cu K $\alpha$  radiation ( $\lambda = 1.54 \text{ \AA}$ ).
- Thermogravimetric analysis (TGA) measurements were performed on Rigaku thermal plus evo2 (TG 8121) under nitrogen atmosphere with the flow rate of  $100 \text{ cm}^3 \text{ min}^{-1}$  and the ramping rate of  $10 \text{ }^\circ\text{C min}^{-1}$ .
- Morphology and particle size were analyzed with a field-emission scanning electron microscope (FE-SEM, JEOL, JSM-7610F) at a low energy (0.8–2.0 keV, in gentle beam mode). The samples were spread on the carbon tape, attached on the sample holder, and spluttered with Platinum at 10 mA for 20 sec to increase the surface conductivity before the measurement.
- Fourier transform infrared (FT-IR) spectra were recorded using a Frontier FT-IR spectrometer (PerkinElmer) in the range of  $400 \text{ cm}^{-1}$  to  $4000 \text{ cm}^{-1}$  with universal attenuated total reflectance (ATR) probe.
- X-ray photoelectron spectroscopy (XPS) was recorded on JEOL JPS-9010MC with a Mg K $\alpha$  source (1,253.6 eV) at 12 kV and 25 mA. All XPS spectra were measured under a high vacuum pressure of  $10^{-8} \text{ Pa}$  at a room temperature. Software for running experiment is SpecSurf ver.1.9.3. The carbon tape was coated with powder samples. The analyzed area of each sample was a circle spot with a diameter of 6 mm. The survey scan spectra were measured with a pass energy of 50 eV, a binding energy range of 0–1,100 eV and an energy step of 1 eV. The narrow scan spectra were measured with a pass energy of 10 eV and an energy step of 0.1 eV. The obtained spectra were evaluated using JEOL software to obtain the chemical state of the probing elements and elemental composition. All the binding energy values were referenced to the carbon peak C1s at 284.7 eV. Note that to avoid the effect of high vacuum operating conditions on the oxidation state of Cu, the analysis on Cu peak was not included.
- Inductively coupled plasma optical emission spectrometry (ICP-OES) was carried out using an Agilent 725 to determine the metal content of the sample. Argon was used as carrier gas and to create the plasma. 0.1 mL of sample was diluted to 10 mL in DI water prior to measurement.  $\text{CuCl}_2 \cdot 2\text{H}_2\text{O}$  was used as a standard for calibration at wavelength of 327.395 nm.

- The utilization efficiency of H<sub>2</sub>O<sub>2</sub> was determined by redox titration of the reaction solution with potassium permanganate (KMnO<sub>4</sub>). Note that to measure the exact concentration of KMnO<sub>4</sub>, the titer determination is performed by titration with 2.5 mM di-sodium oxalate prior to use. In this experiment, 0.96 mM KMnO<sub>4</sub> was used as a titrant for determining H<sub>2</sub>O<sub>2</sub> amount. 0.1 mL of liquid-phase obtained after reaction at 70°C for 4 h was diluted in DI water to 10 mL and was titrated with the prepared KMnO<sub>4</sub>. The titration was repeated at least 3 times. The calculation was done based on these equations.

1. Titer determination:



2. Hydrogen peroxide content determination:



- GC-MS analysis was performed on a GC Clarus 680 (PerkinElmer, Inc., Shelton, Connecticut, USA) equipped with MS Clarus SQ 8T and DB-VRX capillary column (20 m length with a 0.18 mm i.d.; Agilent Technologies, USA). Analysis parameters were as follows: initial temperature = 35 °C, initial time = 5 min, ramping rate = 10 °C min<sup>-1</sup>, final temperature = 200 °C, final time = 3 min. Elution times (min) = 4.13 (CyH); 7.38 (**1**); 7.79 (**3**); 8.86 (**4**); and 11.64 (**2**).

**Table S1.** Effect of reaction temperature on the catalytic performance of Cu-trz catalyst. Reaction condition: Catalyst 25 mg; CyH 200  $\mu$ L; H<sub>2</sub>O<sub>2</sub> (30 %wt.) 250  $\mu$ L; MeCN 2 mL; 4h.

| Reaction temperature (°C) | %CyH conversion | %Oxide (1)  | %Diol (2)   | %1-ol (3)    | %1-one (4)   | %Allylic (3+4) | %Allylic selectivity |
|---------------------------|-----------------|-------------|-------------|--------------|--------------|----------------|----------------------|
| 50                        | 23 $\pm$ 2.7    | 1 $\pm$ 0.1 | n/a         | 3 $\pm$ 0.9  | 6 $\pm$ 2.0  | 8 $\pm$ 2.9    | 94 $\pm$ 2.3         |
| 60                        | 49 $\pm$ 4.9    | 4 $\pm$ 0.5 | n/a         | 7 $\pm$ 0.7  | 19 $\pm$ 3.0 | 26 $\pm$ 3.7   | 87 $\pm$ 1.7         |
| 70                        | 59 $\pm$ 1.2    | 4 $\pm$ 0.3 | 1 $\pm$ 0.2 | 10 $\pm$ 0.4 | 21 $\pm$ 0.5 | 31 $\pm$ 0.6   | 87 $\pm$ 0.4         |

**Table S2.** Effect of reaction time on the catalytic performance of Cu-trz catalyst. Reaction condition: Catalyst 25 mg; CyH 200  $\mu$ L; H<sub>2</sub>O<sub>2</sub> (30 %wt.) 250  $\mu$ L; MeCN 2 mL; 70 °C.

| Reaction time (h) | %CyH conversion | %Oxide (1)  | %Diol (2)   | %1-ol (3)    | %1-one (4)   | %Allylic (3+4) | %Allylic selectivity |
|-------------------|-----------------|-------------|-------------|--------------|--------------|----------------|----------------------|
| 1                 | 28 $\pm$ 3.2    | 1 $\pm$ 0.3 | n/a         | 4 $\pm$ 1.6  | 8 $\pm$ 2.1  | 12 $\pm$ 3.7   | 91 $\pm$ 0.9         |
| 2                 | 48 $\pm$ 1.4    | 3 $\pm$ 0.2 | n/a         | 7 $\pm$ 0.3  | 15 $\pm$ 0.8 | 22 $\pm$ 1.1   | 88 $\pm$ 0.6         |
| 4                 | 59 $\pm$ 1.2    | 4 $\pm$ 0.3 | 1 $\pm$ 0.2 | 10 $\pm$ 0.4 | 21 $\pm$ 0.5 | 31 $\pm$ 0.6   | 87 $\pm$ 0.4         |
| 6                 | 60 $\pm$ 4.6    | 3 $\pm$ 0.5 | 1 $\pm$ 0.3 | 10 $\pm$ 0.6 | 21 $\pm$ 2.5 | 31 $\pm$ 2.9   | 87 $\pm$ 0.5         |
| 12                | 61 $\pm$ 2.3    | 3 $\pm$ 0.1 | 2 $\pm$ 0.7 | 11 $\pm$ 1.9 | 24 $\pm$ 1.6 | 35 $\pm$ 0.5   | 88 $\pm$ 1.4         |
| 24                | 66 $\pm$ 3.5    | 2 $\pm$ 0.4 | 3 $\pm$ 0.6 | 11 $\pm$ 1.1 | 26 $\pm$ 3.2 | 36 $\pm$ 4.3   | 89 $\pm$ 0.4         |

**Table S3.** Effect of catalyst amount on the catalytic performance of Cu-trz catalyst. Reaction condition: CyH 200  $\mu$ L; H<sub>2</sub>O<sub>2</sub> (30 %wt.) 250  $\mu$ L; MeCN 2 mL; 70 °C; 4h.

| Cat. amount (mg) | %CyH conversion | %Oxide (1)  | %Diol (2)   | %1-ol (3)    | %1-one (4)   | %Allylic (3+4) | %Allylic selectivity |
|------------------|-----------------|-------------|-------------|--------------|--------------|----------------|----------------------|
| 0                | <1              | n/a         | n/a         | n/a          | n/a          | n/a            | n/a                  |
| 15               | 58 $\pm$ 6.7    | 3 $\pm$ 0.6 | 1 $\pm$ 0.6 | 8 $\pm$ 2.8  | 17 $\pm$ 4.6 | 25 $\pm$ 7.2   | 85 $\pm$ 1.8         |
| 25               | 59 $\pm$ 1.2    | 4 $\pm$ 0.3 | 1 $\pm$ 0.2 | 10 $\pm$ 0.4 | 21 $\pm$ 0.5 | 31 $\pm$ 0.6   | 87 $\pm$ 0.4         |
| 50               | 55 $\pm$ 5.2    | 3 $\pm$ 0.5 | 1 $\pm$ 0.6 | 9 $\pm$ 1.6  | 22 $\pm$ 2.9 | 31 $\pm$ 1.4   | 88 $\pm$ 1.5         |

**Table S4.** Effect of H<sub>2</sub>O<sub>2</sub> amount on the catalytic performance of Cu-trz catalyst. Reaction condition: CyH 200  $\mu$ L; H<sub>2</sub>O<sub>2</sub> (30 %wt.); MeCN 2 mL; 70 °C; 4h.

| H <sub>2</sub> O <sub>2</sub> ( $\mu$ L) | %CyH conversion | %Oxide (1)  | %Diol (2)   | %1-ol (3)    | %1-one (4)   | %Allylic (3+4) | %Allylic selectivity |
|--|-----------------|-------------|-------------|--------------|--------------|----------------|----------------------|
| 100                                      | 32 $\pm$ 6.6    | 2 $\pm$ 0.2 | n/a         | 13 $\pm$ 1.3 | 11 $\pm$ 1.6 | 24 $\pm$ 2.8   | 94 $\pm$ 0.4         |
| 175                                      | 46 $\pm$ 0.8    | 3 $\pm$ 0.1 | n/a         | 11 $\pm$ 0.9 | 16 $\pm$ 0.7 | 27 $\pm$ 1.6   | 90 $\pm$ 0.4         |
| 250                                      | 59 $\pm$ 1.2    | 4 $\pm$ 0.3 | 1 $\pm$ 0.2 | 10 $\pm$ 0.4 | 21 $\pm$ 0.5 | 31 $\pm$ 0.6   | 87 $\pm$ 0.4         |
| 375                                      | 62 $\pm$ 2.5    | 5 $\pm$ 0.4 | 2 $\pm$ 0.5 | 8 $\pm$ 0.9  | 24 $\pm$ 2.9 | 32 $\pm$ 3.4   | 83 $\pm$ 1.8         |

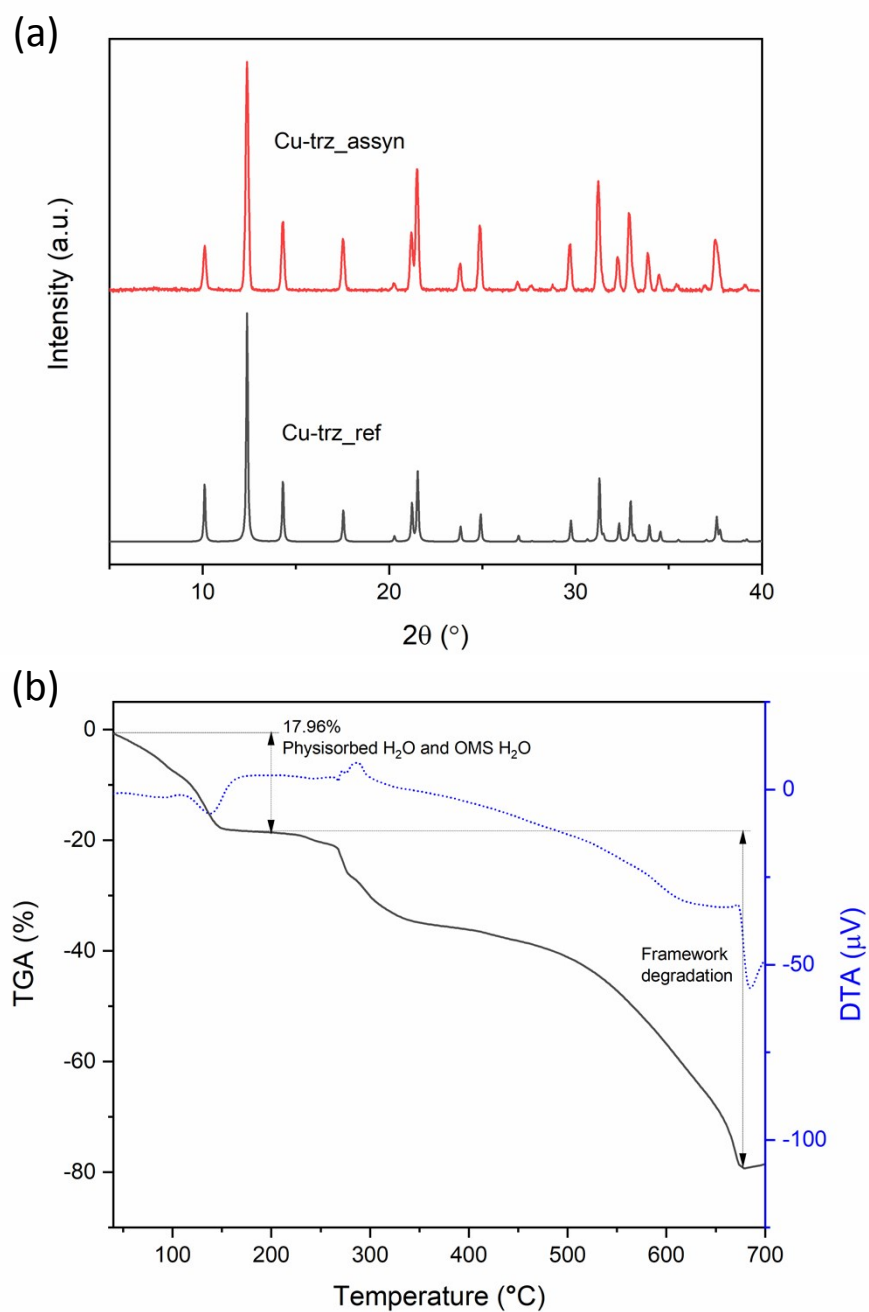


**Figure S1.** (a) PXRD patterns of simulated<sup>1</sup> and as-synthesized Cu-trz, and (b) TGA and DTA curves of as-synthesized Cu-trz measured under  $\text{N}_2$ .

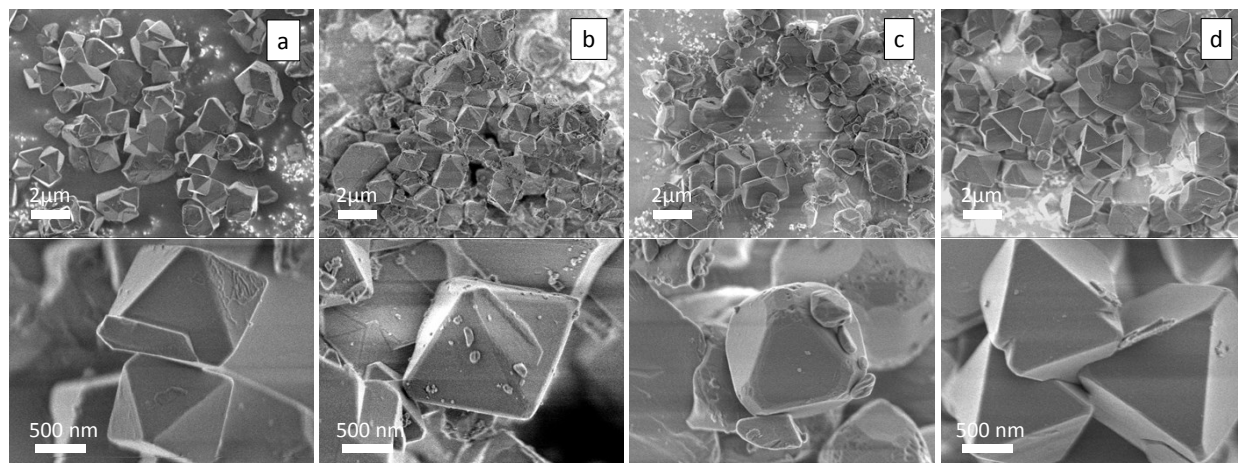


**Figure S2.** SEM images of (a) as-synthesized Cu-trz and Cu-trz after immersed in aqueous solutions of (b) NaOH (pH 10), (c) HNO<sub>3</sub> (pH 2), and (d) H<sub>2</sub>O<sub>2</sub> (30 %wt.) for 24 h.

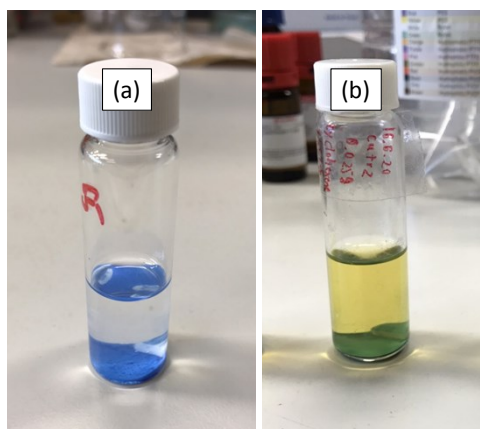


**Figure S3.** Solution mixtures (a) before and (b) after oxidation of CyH at 50 °C for 24h.

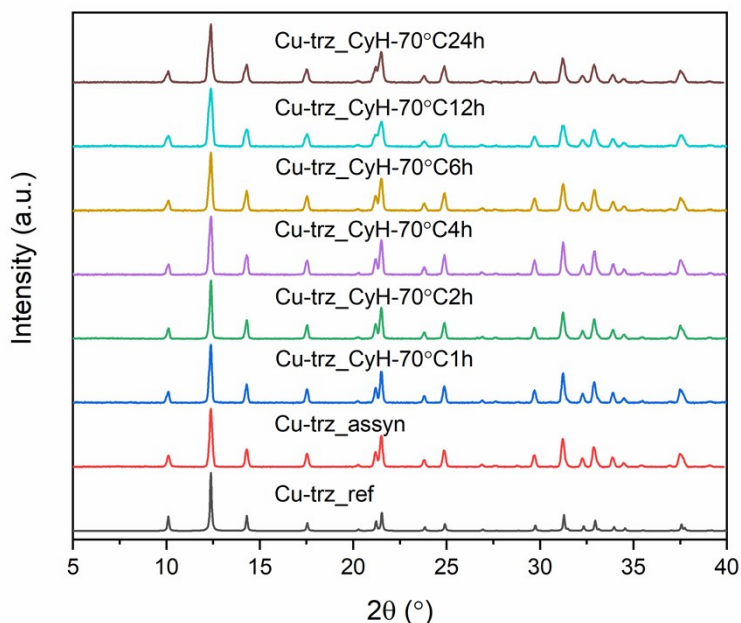


**Figure S4.** PXRD patterns of simulated<sup>1</sup> and as-synthesized Cu-trz, and Cu-trz after oxidation of CyH at 70 °C with varied reaction times.

: The broader full width at half maximum (FWHM) of PXRD peaks was observed from the catalyst reacting for more than 12 h, indicating reduced crystallinity due to the long reaction time.

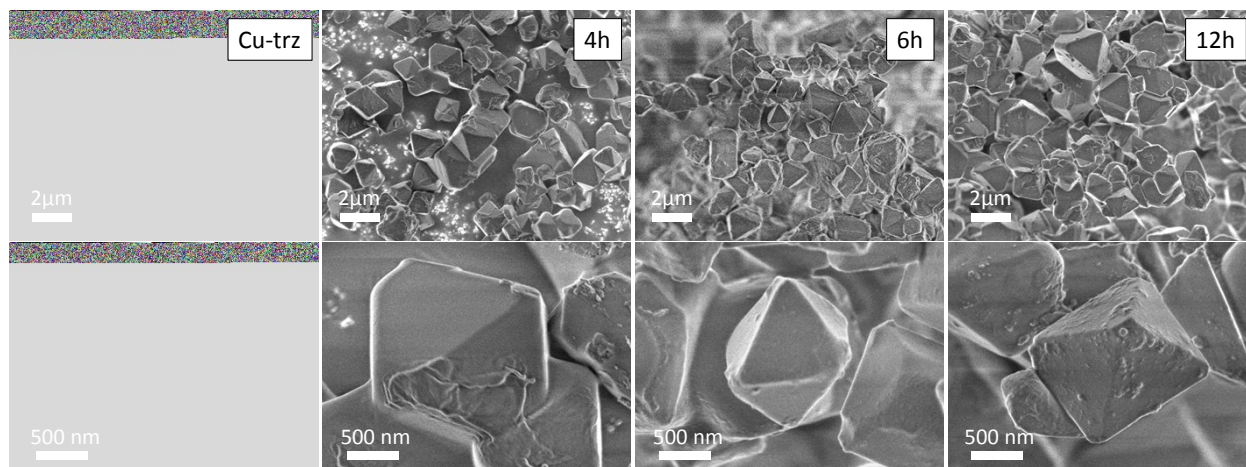


**Figure S5.** SEM images of as-synthesized Cu-trz and Cu-trz after oxidation of CyH at 70 °C with varied reaction times.

: The SEM images of Cu-trz after the reactions showed the preserved morphology as compared to the as-synthesized compound, indicating the high stability of the framework.

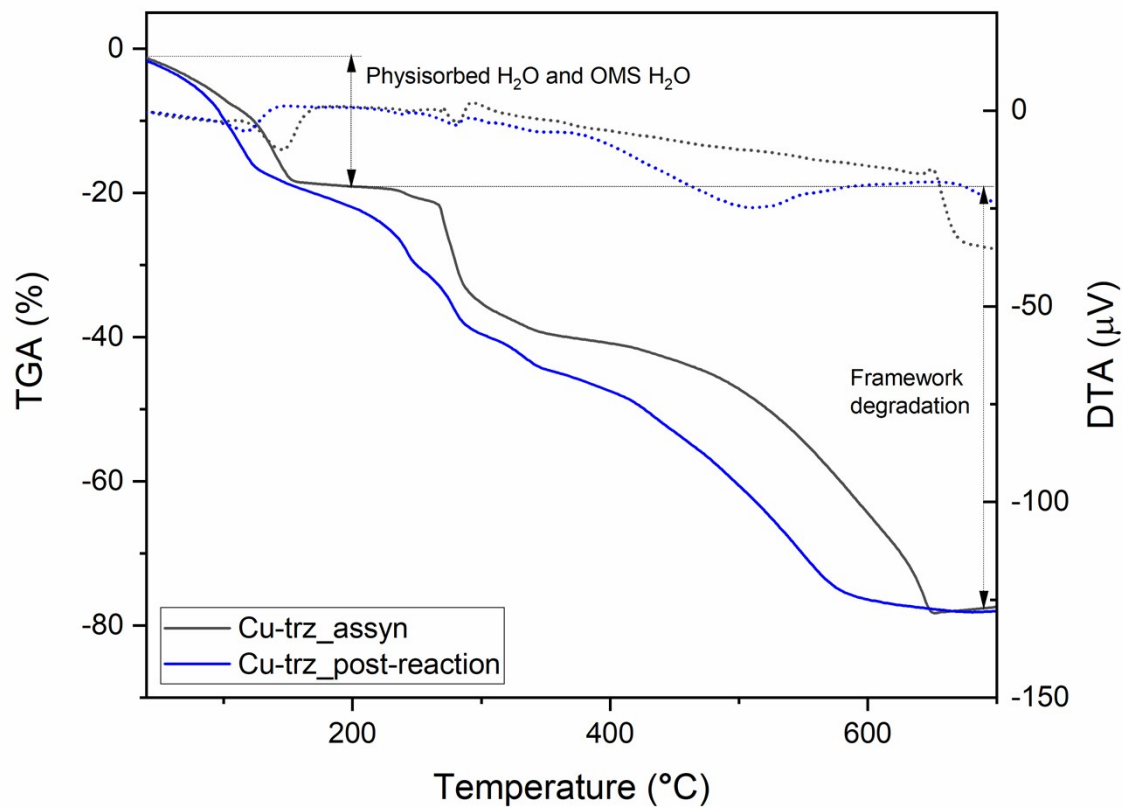
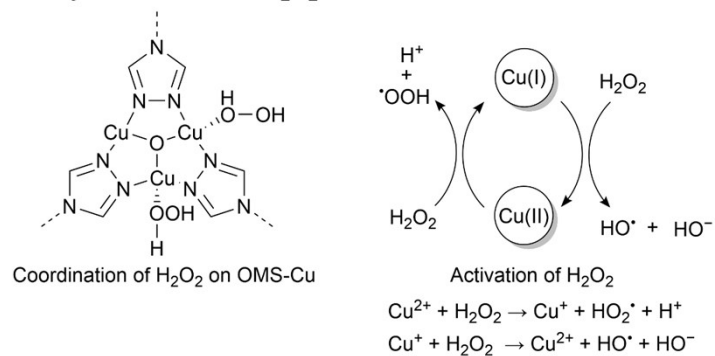
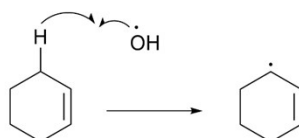


**Figure S6.** TGA (solid line) and DTA (dotted line) curves of as-synthesized Cu-trz and Cu-trz after oxidation of CyH.

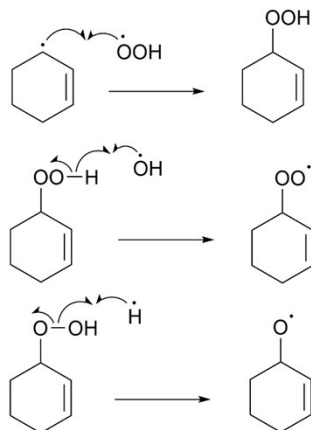
### Homolytic Activation of H<sub>2</sub>O<sub>2</sub>



### Initiation



### Propagation



### Termination

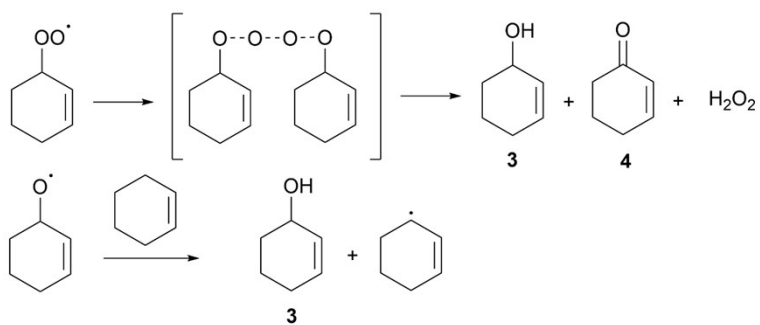


**Figure S7.** Proposed reaction mechanism for the oxidation of CyH over Cu-trz MOF via homolytic cleavage of H<sub>2</sub>O<sub>2</sub>.

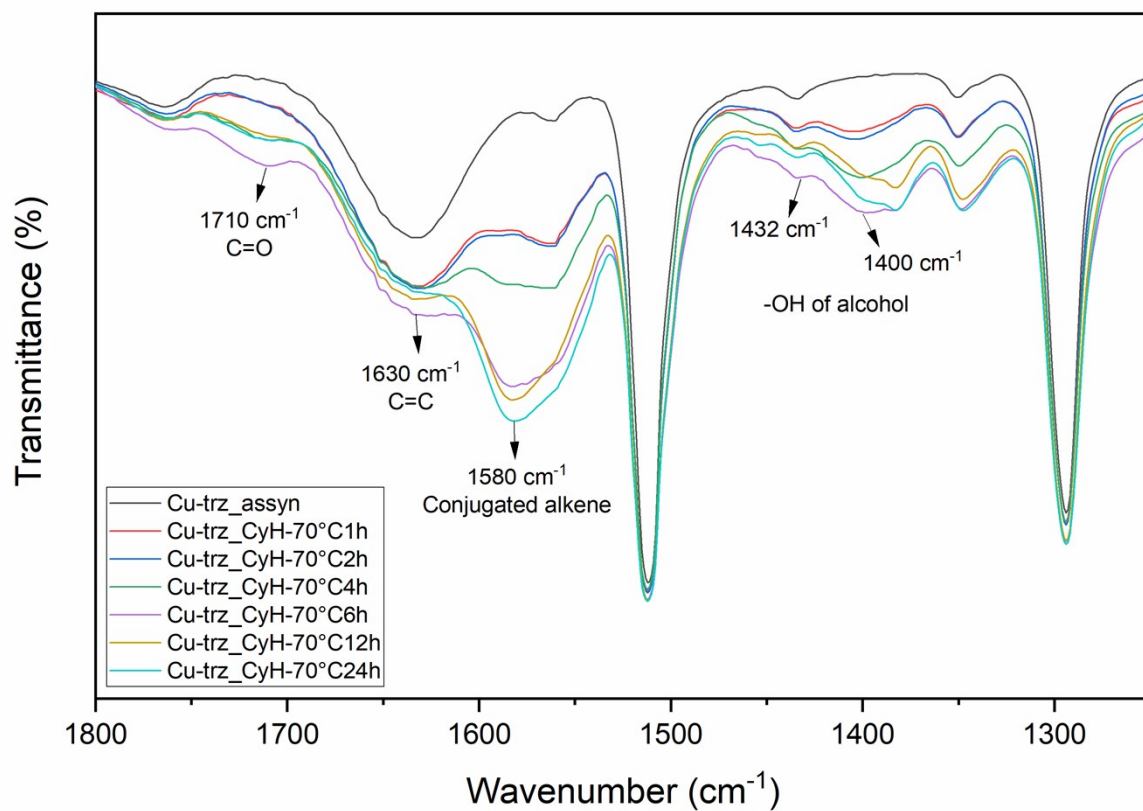


**Figure S8.** FT-IR spectra of as-synthesized Cu-trz and Cu-trz after oxidation of CyH at 70 °C with varied reaction times.

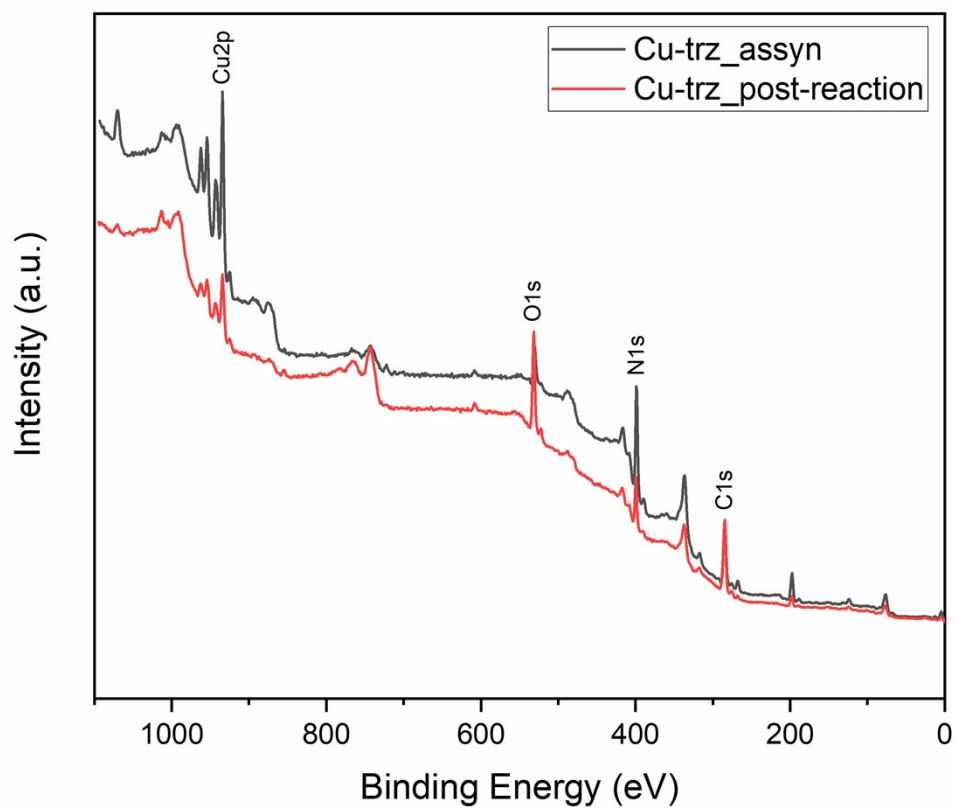


**Figure S9.** Wide scan XPS spectra of as-synthesized Cu-trz (black) and Cu-trz after oxidation of CyH at 70 °C for 1 day (red).

: The wide scan XPS spectra contain Cu, O, and N elements at binding energy positions of 934 eV, 530 eV, and 398 eV, respectively.

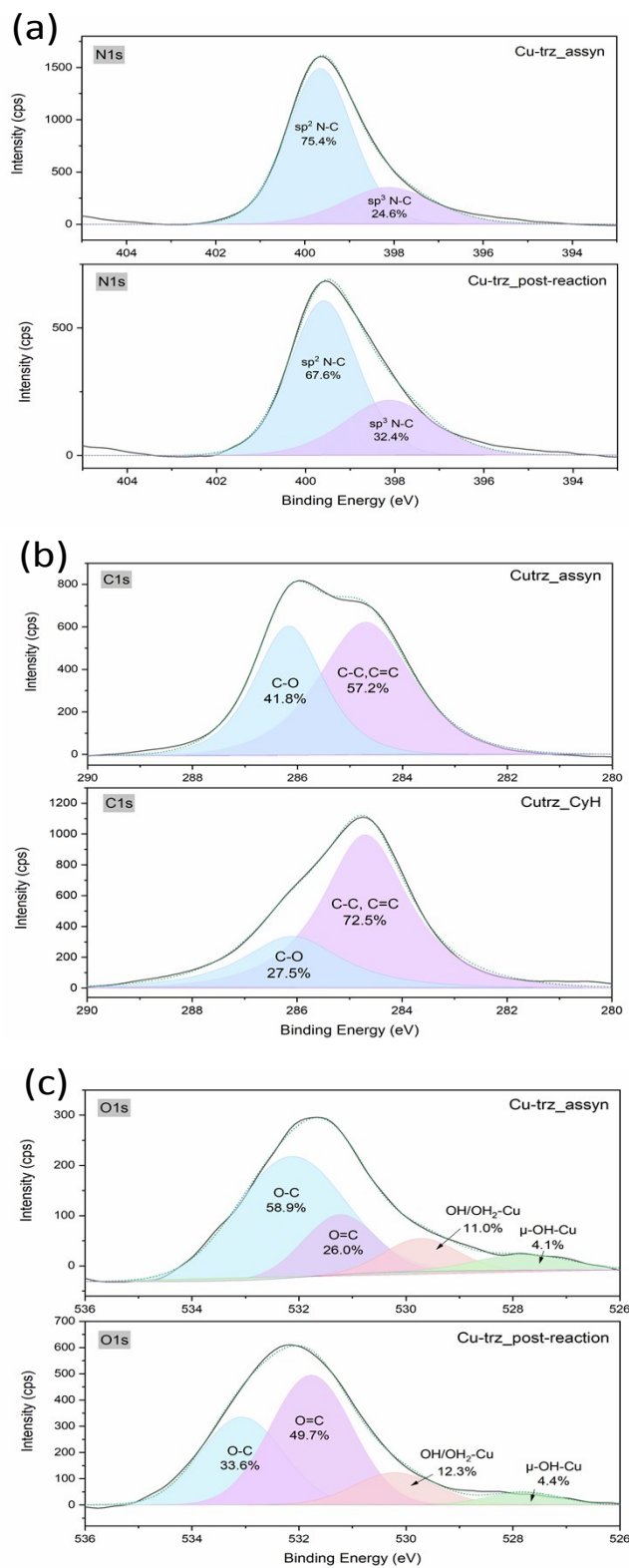


**Figure S10.** Deconvoluted XPS spectra for (a) N1s, (b) C1s, and (c) O1s of Cu-trz and Cu-trz after oxidation of CyH at 70 °C for 1 day.

**Table S5.** %Cu leaching in the liquid phase after oxidation of CyH for 1, 2, 4, 6, 12, and 24 h according to ICP-OES measurement. (Standard =  $\text{CuCl}_2 \cdot 2\text{H}_2\text{O}$ ,  $\lambda = 327.395 \text{ nm}$ ,  $R^2 = 0.9998$ )

| Reaction time (h) | %Cu-leaching |
|-------------------|--------------|
| 1                 | 1.8          |
| 2                 | 2.1          |
| 4                 | 2.5          |
| 6                 | 6.7          |
| 12                | 14.1         |
| 24                | 16.3         |

: The direct elemental analysis using inductively coupled plasma optical emission spectroscopy (ICP-OES) was carried out. The ICP-OES results of liquid phase after the reaction at 70 °C for 1 h to 24 h was shown in Table S5. At longer reaction times, Cu-leaching amount gradual increased. Under the optimized condition of 4h, the reaction showed only small amount of Cu-leaching of 2.5%.

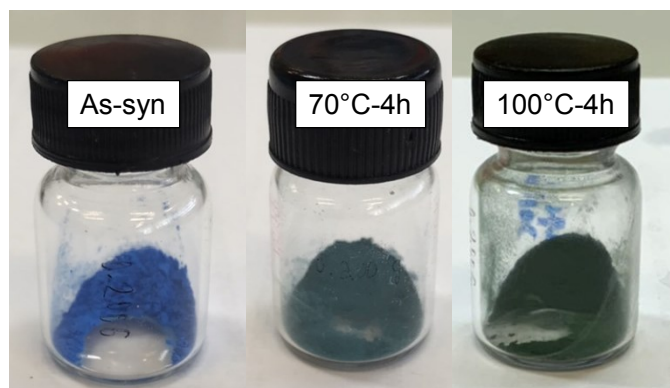


**Figure S11.** Powder color of as-synthesized Cu-trz and Cu-trz activated under reduced pressure at temperatures of 70 °C and 100 °C for 4h.

: Thermal activation at 70 °C and 100 °C was applied to Cu-MOF prior to the catalytic reaction. Photographs of the as-synthesized and activated solids were shown in Figure S11. The blue powder (as-synthesized form) turned to dark green under thermal activation, confirming the de-coordination of water from the framework. This suggested that the Lewis acid sites can be generated at the reaction temperature of 70 °C.

**Table S6.** Catalytic activity of the Cu-MOF activated at different temperatures under reduced pressure. Reaction condition: CyH 200  $\mu$ L; H<sub>2</sub>O<sub>2</sub> (30 %wt.) 250  $\mu$ L; MeCN 2 mL; 70 °C; 4h.

| Sample         | %CyH conversion | %Oxide (1) | Diol (2) | %1-ol (3) | %1-one (4) | %Allylic (3+4) | %Allylic selectivity |
|----------------|-----------------|------------|----------|-----------|------------|----------------|----------------------|
| As-synthesized | 59              | 4          | 1        | 10        | 21         | 31             | 87                   |
| 70°C-4h        | 61              | 4          | 1        | 10        | 26         | 36             | 87                   |
| 100°C-4h       | 61              | 4          | 1        | 11        | 27         | 38             | 87                   |

: The activated frameworks were subjected to the catalytic reaction at optimized condition and compared with that of the as-synthesized one. The catalytic activities were described in Table S6. The results revealed that the thermal activation of the catalyst did not play significant role to the CyH conversion while the allylic yields were improved slightly. This supported that the water in H<sub>2</sub>O<sub>2</sub> oxidant could competitively coordinate at the Lewis OMS-Cu center, resulting in insignificant improvement in allylic production (only 7%).

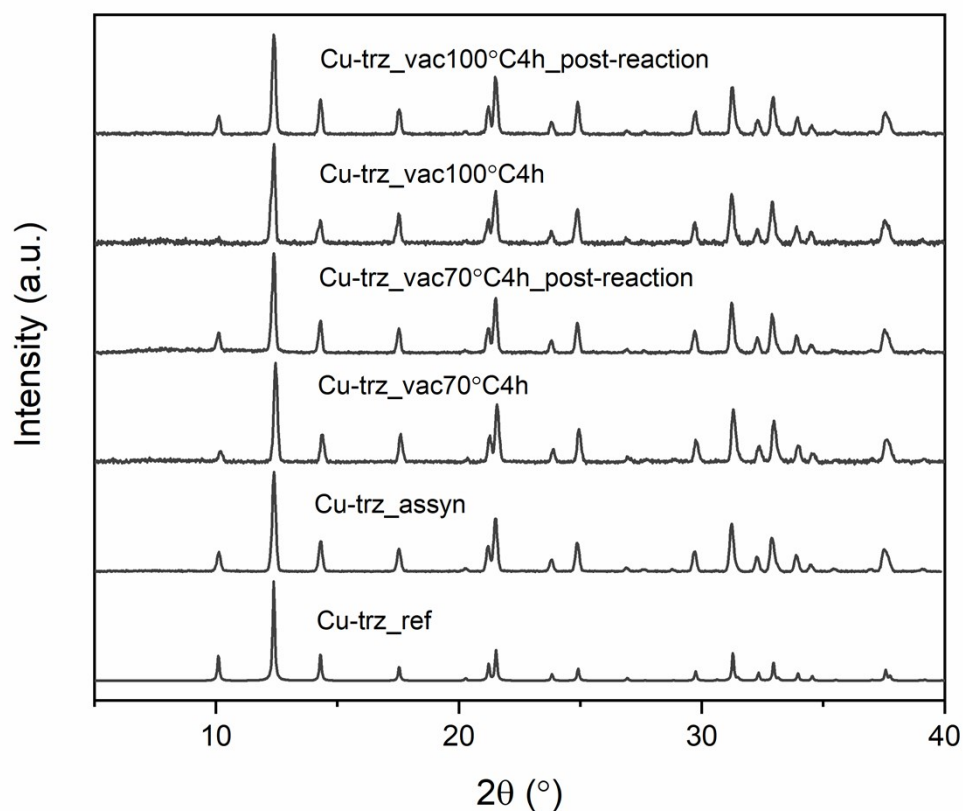


**Figure S12.** PXRD patterns of simulated<sup>1</sup>, as-synthesized Cu-trz, and activated Cu-trz before and after oxidation of CyH at 70 °C for 4h.

: Upon the thermal activation generating OMS-Cu, the structural integrity of Cu-trz was maintained. Also, the PXRD patterns of used catalysts from the oxidation of CyH with H<sub>2</sub>O<sub>2</sub> remained unchanged, suggesting the high stability of the framework toward the reaction.

**Table S7.** Effect of catalyst filtration on the catalytic performance of Cu-trz MOF. Reaction condition: CyH 200  $\mu$ L; H<sub>2</sub>O<sub>2</sub> (30 %wt.) 250  $\mu$ L; MeCN 2 mL; 70  $^{\circ}$ C.

| Entry | Cat.      | Reaction Time (h) | %Oxide<br><b>1</b> | %Diol<br><b>2</b> | %1-ol<br><b>3</b> | %1-one<br><b>4</b> | %Allylic<br><b>3+4</b> |
|-------|-----------|-------------------|--------------------|-------------------|-------------------|--------------------|------------------------|
| 1     | Cu-trz    | 1                 | 1 $\pm$ 0.3        | n/a               | 4 $\pm$ 1.6       | 8 $\pm$ 2.1        | 12 $\pm$ 3.7           |
| 2     | Cu-trz    | 2                 | 3 $\pm$ 0.2        | n/a               | 7 $\pm$ 0.3       | 15 $\pm$ 0.8       | 22 $\pm$ 1.1           |
| 3     | Cu-trz    | 4                 | 4 $\pm$ 0.3        | 1 $\pm$ 0.2       | 10 $\pm$ 0.4      | 21 $\pm$ 0.5       | 31 $\pm$ 0.6           |
| 4     | Cu-trz    | 6                 | 3 $\pm$ 0.5        | 1 $\pm$ 0.3       | 10 $\pm$ 0.6      | 21 $\pm$ 2.5       | 31 $\pm$ 2.9           |
| 5     | Cu-trz    | 12                | 3 $\pm$ 0.1        | 2 $\pm$ 0.7       | 11 $\pm$ 1.9      | 24 $\pm$ 1.6       | 35 $\pm$ 0.5           |
| 6     | Filtrate* | 2                 | 1 $\pm$ 0.1        | n/a               | 4 $\pm$ 0.3       | 8 $\pm$ 0.5        | 12 $\pm$ 0.8           |
| 7     | Filtrate* | 4                 | 2 $\pm$ 0.2        | n/a               | 6 $\pm$ 0.6       | 10 $\pm$ 1.0       | 16 $\pm$ 1.6           |
| 8     | Filtrate* | 6                 | 2 $\pm$ 0.2        | n/a               | 6 $\pm$ 0.8       | 11 $\pm$ 1.4       | 17 $\pm$ 2.1           |
| 9     | Filtrate* | 12                | 2 $\pm$ 0.1        | n/a               | 6 $\pm$ 0.3       | 11 $\pm$ 0.6       | 17 $\pm$ 0.9           |

\*The catalyst was filtered off from the reaction mixture after reacting for 1 h and then kept reacting at varied reaction times.

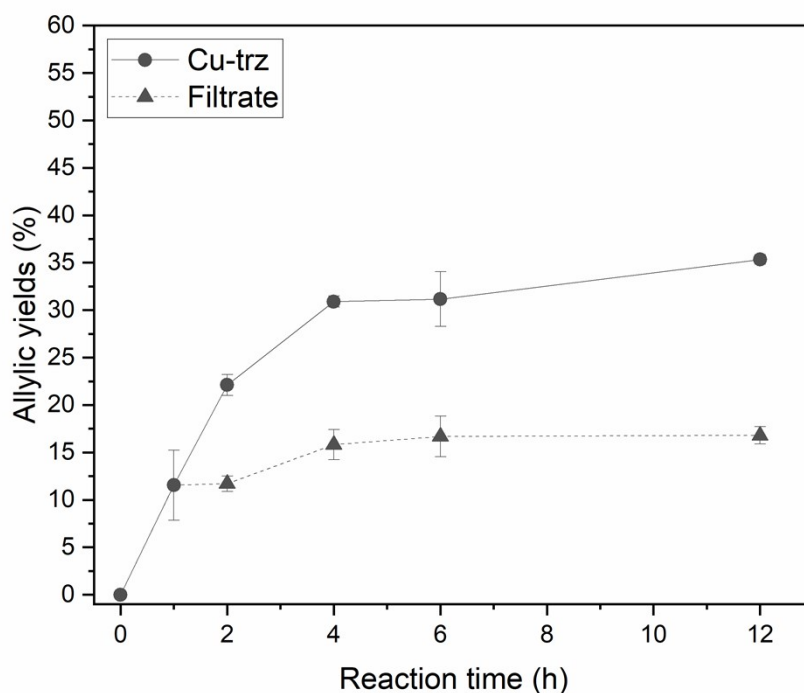


**Figure S13.** Kinetic profiles for the allylic-product accumulation with and without catalyst separation by hot filtration at 70  $^{\circ}$ C-1h.

: The hot filtration test was performed on the CyH oxidation reaction over Cu-trz catalyst. To avoid the re-adsorption of active species, the filtrations were carried out at the elevated temperature of 70  $^{\circ}$ C. Reaction mixture from the CyH oxidation at ca. 50% of the maximum CyH

conversion (70 °C-1h, Table 1) was filtered and allowed the filtrate to proceed the reaction further to 12 h (Table S7). Kinetic profiles of the reactions with and without catalyst by hot-filtration method were illustrated in and Figure S13. The reactions of the filtrates (Entry 6-9) showed slight improvement in allylic yields as compared with that of the reaction with Cu-trz catalyst for 1 h (Entry 1). The slightly increased allylic yield may be affected by the small Cu<sup>2+</sup> leached out from the framework, supported by ICP-OES results (Table S5). The results indicated that albeit its high stability of solid Cu-trz catalyst, Cu metal leaching from the framework upon CyH oxidation at high temperature was unavoidable.

However, the allylic yields from the reaction of the filtrates were far inferior to those of the reactions with the presence of Cu-trz catalyst at the similar reaction conditions. In addition, the allylic yields from the reaction with Cu-trz at prolonged reaction times, *e.g.* 6 h and 12 h with high Cu-leaching, did not increase significantly. This suggested that the metal leached from Cu-trz may not be major active species for the reaction. This can be concluded that the CyH oxidation over Cu-trz MOF in the present work mainly occurred through the heterogeneous catalysis.

#### Reference.

1. T. Yamada, G. Maruta and S. Takeda, *Chem. Commun.*, 2011, **47**, 653-655.